The Image-to-Physical Liver Registration Sparse Data Challenge

E. Lee Brewer[a], Logan W. Clements[b,c], Jarrod A. Collins[b,c], Derek J. Doss[b,c], Jon S. Heiselman[b,c], Michael I. Miga[b,c,*], Chris D. Pavas[d], and Edward H. Wisdom III[a]
[a]Vanderbilt University Information Technology, Vanderbilt University, Nashville, TN, US, [b]Vanderbilt University, Department of Biomedical Engineering, Nashville, TN, US, [c]Vanderbilt Institute for Surgery and Engineering, Nashville, TN, USA, [d]Tennessee State University, Department of Computer Science, Nashville, TN, USA
*Corresponding Author (authors listed alphabetically)

ABSTRACT

Over the last 25 years, the number of papers written that involve image guidance, liver, and registration has, on average, doubled every 6-8 years. While image guidance has a long history within the neurosurgical theatre, it's translation to other soft-tissue organs such as the liver has been slower given the inherent difficulty in image-to-physical registration. More specifically, deformations have been recognized to compromise image guidance fidelity in virtually all soft-tissue image guidance applications. As a result, an active area of investigation is the development of sparse-data-driven nonrigid image-to-physical liver registration techniques to compensate for deformation and provide accurate localization for image guided liver surgery. In this work we have leveraged our extensive human-to-phantom registration testing framework based on the work in [1] and Amazon Web Services to create a sparse data challenge for the image guided liver surgery community (https://sparsedatachallenge.org/). Our sparse data challenge will allow research groups from across the world to extensively test their approaches on common data and have quantitative accuracy measurements provided for assessment of fidelity. Welcome to the Sparse Data Challenge for image-to-physical liver registration assessment.

Keywords: registration, deformation, liver, nonrigid, finite element, image guidance, challenge

1. INTRODUCTION

1.1 Background

In recent years, the resolve to move image guided techniques within the abdomen has accelerated. With the most recent advances in navigational safety, resection indications have expanded to patients with more advanced disease. Wedge resections, resection of multiple segments, resection combined with ablation, and two-stage resection are being performed with greater frequency [2, 3]. In addition, this has spurred advances in surgical delivery and is expanding indications for less invasive conventional and robot-assisted laparoscopic liver surgery [4], both of which are associated with less blood loss, lower morbidity, less complications, shorter length of stay, and lower cost [5]. As a consequence, re-operations are becoming less difficult (e.g. laparoscopic re-hepatectomy [6]), thus remarkably enabling less invasive surgery to become a neoadjuvant treatment for those awaiting transplant [7]. In addition, when considering the expanding adjuvant role of locoregional therapies (e.g. thermal ablation or irreversible electroporation) [8], truly dynamic treatment options are emerging for liver surgical therapy.

Central to this translation is the registration of the wealth of preoperative imaging information to the physical space associated with the patient. Within the domain of open and laparoscopic surgery, the primary tools of localization have been associated with three dimensional digitizers (e.g. optical tracking, electromagnetic digitizers, etc), computer vision based systems (e.g. laser range scanning, stereo pair cameras, etc), and intraoperative imaging (primarily ultrasound, and to a lesser degree cone-beam computed tomography). As a result of the more constrained surgical environment, image-to-physical registrations are usually accomplished with an organ-based registration using surface data, subsurface vasculature geometries, or combinations of two data streams [9-14]. Given the availability of the organ surface during procedures (open and laparoscopic) and the advances in vision-based digitization strategies, it seems likely that organ surface data will be utilized in the future. As a result, we have designed a sparse-data challenge that involves the acquisition of unstructured point cloud data taken of a mock liver surface in a series of deformed states both with and without added digitization noise and with varied data surface extents reflective of experiences in the operating room (OR). More specifically, these data patterns are based on real physical swabbings of patient livers done with a tracked stylus in previous work [1, 15, 16]. In addition, in [16], these swabbings were collected within strict time limitations as it is the only study to our knowledge that has tested deformation correction within the OR in *real time*.

1.2 Purpose

The purpose of this paper is present our sparse data challenge to the liver registration community. Briefly described, the challenge is based on the publication by Collins et al. (2017) appearing in the *IEEE Transactions on Medical Imaging* (vol. 36, no. 7, pp. 1502-1510) [1]. The underlying rationale is that there are surgical workflow advantages if one could align preoperative liver image volume data to its intraoperative physical counterpart using sparse surface data visible during the procedure at presentation. We have developed a novel human-to-phantom framework that allows us to transpose real OR data patterns that we acquired clinically using an optically tracked stylus onto a quantitative deforming mock-tissue phantom environment. This framework allows the development and testing of image-to-physical registration algorithms in the presence of deformation with quantitative subsurface targets for assessing error and within the context of realistic OR data acquisition. We note that the deformations we have imposed on the phantom mimic patterns of deformation we have seen in the OR.

2. METHODS

2.1 Platform

To facilitate the challenge, Amazon Web Services (AWS) has been deployed for the development platform (Figure 1). AWS is a cloud computing service that provides a simple way to: provision and access servers, store data, build databases and a broad set of applications services over the internet with a friendly interface. AWS was chosen as the platform for the challenge for 3 reasons: (1) flexibility, (2) security, and (3) presence. With respect to flexibility, AWS provided a variety of options with respect to operating systems, programming languages, web application platform, database, and other services. With respect to security, standard password protection, user-designated submission accounts, and secure file transfers were easily enabled for tracking participants. With respect to presence, one aspect of the sparse data challenge is to encourage use of such services to create similar approaches to challenges around the world. AWS has more than 10 regions, 36 availability zones and more than 50 edge locations allowing for efficient participation.

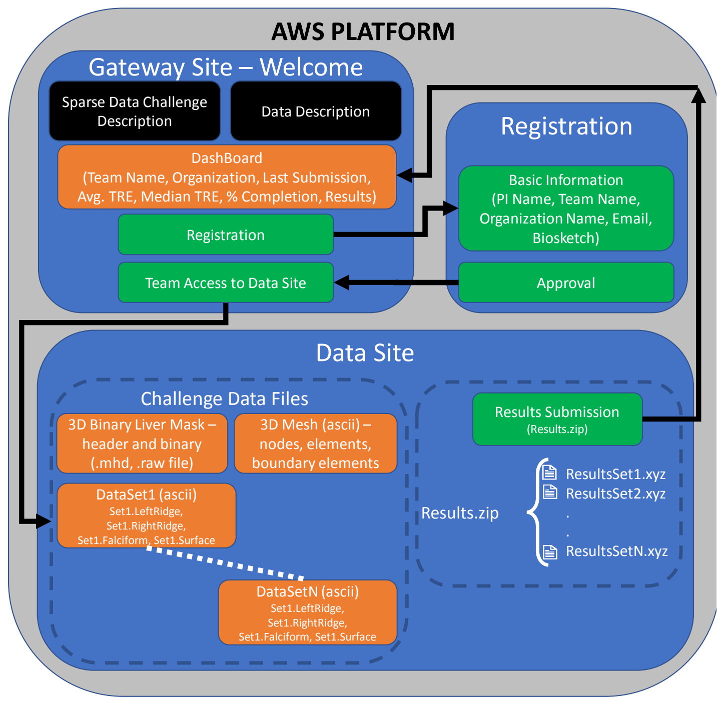

Figure 1. AWS platform management of challenge which includes gateway website, registration, data site.

2.2 Phantom Data Summary

Central to our challenge is the need of a liver shaped phantom with deformation behavior that simulates a mock presentation of the liver during open surgery. The phantom was constructed from 80% Ecoflex® 00-10 platinum-cure silicone mixed with 10% Silicone Thinner® and 10% Slacker® Tactile Mutator (Smooth-On Inc., Pennsylvania) using a patient-specific CT image volume (Figure 2a). Once created, we proceeded to embed 1mm diameter stainless steel beads (n=159) throughout the phantom (Figure 2b). The phantom was then placed back into its mold base which was created from the preoperative patient configuration. The mock liver was then subject to high resolution CT scanning to establish

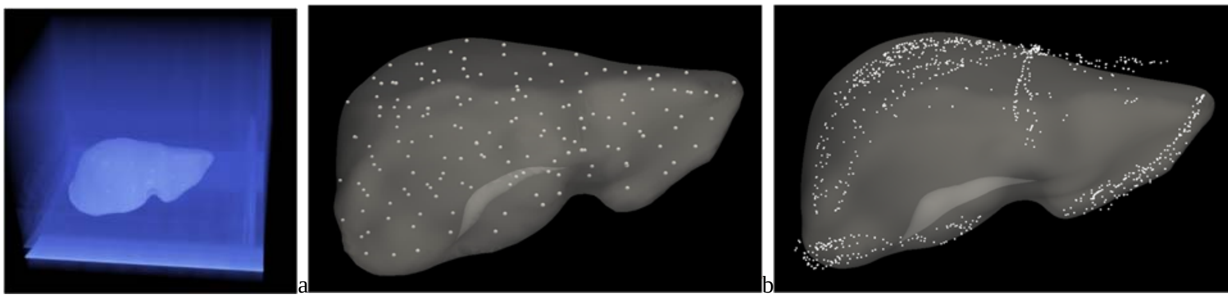

Figure 2. (a) Phantom CT, (b) phantom with embedded bead locations, and (c) sparse data pattern from the operating room superposed on the phantom.

a baseline configuration. Once complete, mock surgical packing was placed under the posterior side of the mock liver with 4 different deformation configurations. With each configuration, repeat CT imaging was performed and deformation quantified by tracking the individual targets.

Once complete, the methods from [1] were utilized to automatically transpose patterns of organ surface swabbing from real operating room cases collected in previous work on to the deformed CT-derived surfaces (Figure 2c). In addition, in order to make these transposed swabbings more realistic, displacement variations in the swab height from the acquired deformed CT-surface were produced to simulate the natural variation in acquisition due to stylus-to-tissue contact changes. Lastly, we should note that our registration methodology, both rigid [17] and nonrigid [18, 19], utilizes the salient features on the liver of the left and right inferior ridge, and falciform ligament region. We provide this data as part of each set. These too are also based on real OR experiences.

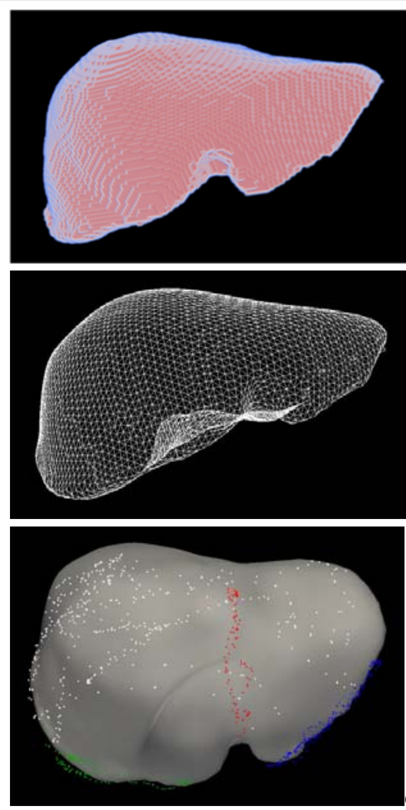

Figure 3. (a) Binary mask, (b) tetrahedral mesh, and (c) surface point collection - blue, green, red, and white points are left inferior ridge, right inferior ridge, falciform ligament, and extra swabbed points, respectively

2.3 Challenge Data

With respect to the data provided in the challenge, a binary image volume mask of the phantom liver in its undeformed state is provided. In addition, a 3D tetrahedral mesh based on that mask in real physical dimensions is provided. The registrant is welcome to use the mesh for their own algorithmic development. Of note, all results will be ultimately reported and assessed on this grid which aligns with the mask in the reporting phase. The last file provided for you is a zip-file of 112 sparse data sets representing real patterns of data from the OR transposed onto our quantitative phantom system. The data consists of 21 different patterns of swabbed data with 4 different deformation states for a total of 84 data sets. In addition, we extracted 7 additional novel data sets that were applied to the 4 different deformation states creating an additional 28 cases of data. This last set was focused at understanding the influence of non-contact digitization. We randomly assigned each of these to one of the four deformation states with the constraint that each state should have only 7 patterns. These cases are used to study algorithm performance in the case of non-contact methods of digitization. With respect to provided data for the challenge, it consists of the following:

Binary Mask (Figure 3a): A header and raw file have been provided. This can be used to build your own representation of the liver domain. The binary mask provided is 512 x 512 x 631 with spacing of 0.683594 x 0.683594 x 0.8 mm. The header file is in ascii while the image volume is stored as a binary raw volume.

3D Tetrahedral Grid (Figure 3b): A 3D tetrahedral domain of the liver phantom in its pre-deformed state has been provided to you. This domain was constructed from the binary mask. It is described by three files: (1) a node file that contains on each line an index and the x, y, and z coordinate of each 3D point, (2) an element file that contains on each line an index followed by 4 integers that represent the node indices that make up each individual tetrahedral element, and (3) a boundary element file that contains on each line an index followed by 3 integers that represent the node indices that make up each surface patch triangle on the exterior surface of the organ. The three files that make up the tetrahedral grid are stored in ascii format.

Zipped Data File (Figure 3c): The zipped data file is a standard zip archive in the MSWindows environment file that contains 112 folders. Each folder has a consistent set of mock intraoperative liver surface data. The data in an individual folder consists of 4 separate ascii point cloud files. Each file is the acquired data from a different portion of the phantom, namely, (1) left inferior ridge, (2) right inferior ridge, (3) falciform region, and (4) general surface swabbing across the surface. The task for the challenge is to align the grid space associated with 3D mesh to that of each sparse data pattern to the best of the participant's algorithm ability. It is your choice whether you use any of the geometric references provided. We provide here because these have been shown to be salient features that physicians can determine relatively easily and without moving the organ in typical presentations. Taking all 4 data files and merging would provide the extent of data acquisition of the anterior liver surface provided. The spatial extent of the liver surface provided in the challenge varies between 20%-44% of the liver surface.

2.4 Challenge Submission

Full submission: A full data submission represents a compressed zip file (use standard zip archive in MSWindows environment) that contains one result file per sparse challenge data set for a total of 112 results files to be used for submission. It is critical that each result file have the following naming convention (name is within the single quote): 'ResultsSet001.xyz', 'ResultsSet002.xyz', 'ResultsSet003.xyz', etc... Each of these would correlate with the first, second, and third sparse data set driven results, and so on, respectively, and would continue until 'ResultsSet112.xyz' for a complete submission. All 112 files should be in ascii format and should be stored in one .zip folder file. With respect to each 'ResultsSet###.xyz' file, each will consist of 7 columns consisting of: an index, x nodal coordinate, y nodal coordinate, z nodal coordinate, displacement of nodal coordinate in x direction, displacement of nodal coordinate in y direction, displacement of nodal coordinate in z direction. We should note that the first 4 columns will be identical to the 4 columns in the provided mesh node file from the download. Once successfully submitted, results will be automatically processed by the embedded AWS processing scripts, and the results will be posted on the submission dashboard shortly thereafter.

Partial submission: We also allow for a partial submission for the purpose of development and accelerating testing for participants. With a partial submission, the notes about the compressed file in the previous section are the same. The primary difference in a partial submission is that only a subset of the 112 results files is submitted in the .zip file. The most important aspect is to ensure that the number reference within 'ResultsSet###.xyz' matches the corresponding number as relayed in the sparse data challenge sets that are utilized to drive the result. Once .zip file containing some results is successfully submitted, results will be automatically processed, and the results will be posted on the dashboard. The dashboard will reflect the percentage of the 112 files submitted in each submission.

3. RESULTS

Table 1 is the quantitative results from our nonrigid registration approach over all 112 data sets with each set yielding n=159 distributed targets.

Target Registration Error Results		
Surface Coverage	Average Target Registration Error (mm)	Median Target Registration Error (mm)
20-28%	4.68 ± 0.86	4.78
28-36%	4.59 ± 1.16	4.42
36-44%	4.29 ± 0.95	4.19
All Data Sets	4.52 ± 1.01	4.44

Table 1. Target registration results for sparse data challenge based on methods from [18].

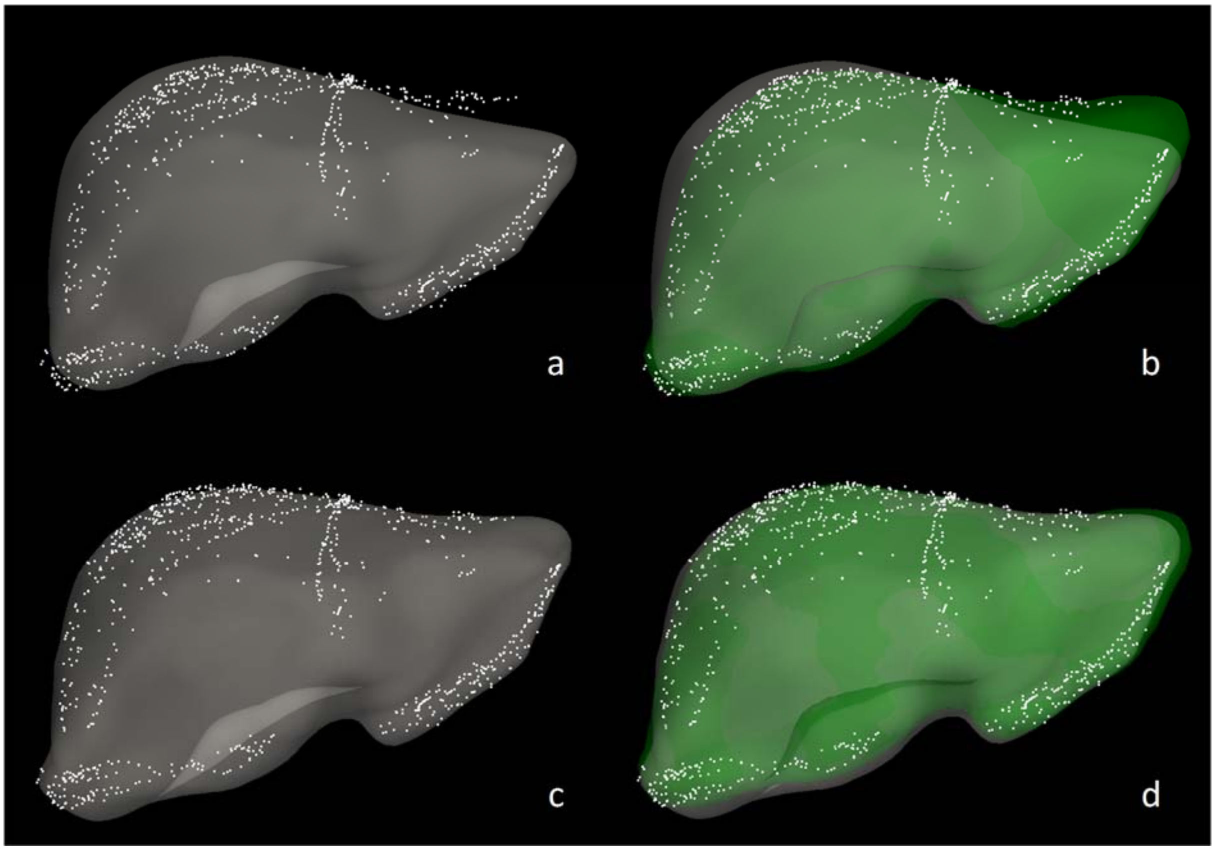

Figure 4. (a) Rigidly aligned pre-deformed liver phantom surface and the acquired swabbed data (white points) after deformation had been applied, (b) same as (a) but the deformed CT data surface used to create sparse point cloud shown. (c,d) are the counterparts of (a,b) but using our nonrigid registration approach.

With respect to the challenge, we have provided the first submission to the site dashboard using our previously published algorithm based in [18] which is an improved algorithm from that of [1, 19]. Additional refinements since [18] have been developed and will be reported in a later manuscript. Figure 4 is a representative registration from one data set. Figure 4a is the alignment of the liver phantom surface prior to the application mock-surgical deformations and the acquired swabbed data (white points) after deformation has been applied. Figure 4b shows the reflective deformed CT surface which is the deriving data for the white points in their deformed state. Figure 4c, 4d is the counterparts for Figure 4a, 4b after the application of our nonrigid registration algorithm. We should note that the initial state of the sparse data is significantly misaligned with respect to image data. The results shown in Figure 4a,b is one step within our multi-step nonrigid registration framework. We provide here for a reference that shows the effect of deformation.

4. DISCUSSION

The structure of the challenge highlighted in Figures 1-3 is unique in the extent of the challenge, and the management and automation of analysis through Amazon Web Services. In addition, the results of our submission for the challenge are quite good (average target registration error less than 5mm) as illustrated from Table 1 and Figure 4. With respect to the nature of deformation in the challenge, the four deformation states span a range of conditions that cover various disease presentations, i.e. some deformations within the set are relatively moderate as is the case where fibrosis is present clinically; while others represent large deformation states and

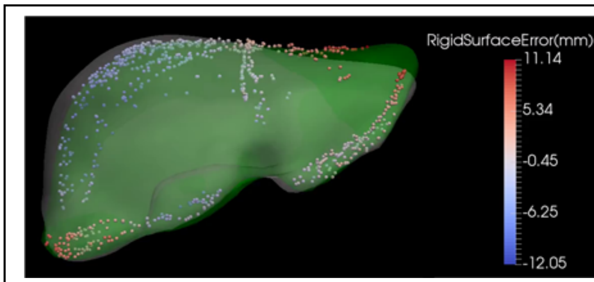

Figure 5. Signed closest point distances after rigid registration in large deformation challenge sets.

have signed closest point distances ranging from -12 to 11 mm after rigid registration (Figure 5). These data are remarkably similar to the extensive clinical data we have reported in [18, 20].

5. CONCLUSION

To our knowledge, this is the only sparse data image-to-physical liver registration challenge that utilizes sparse surface data based on real operating room digitization experiences. In addition, the extensive nature of that data employs 4 different deformation states, 3 different data extents, and 7 OR contact-based swabbing patterns for each extent which leads to 84 data registration challenges for participants. In addition, we have added another 28 sets that allow for performance evaluations within the context of non-contact surface data acquisition. Finally, with all these data, the site simultaneously provides a framework to allow for quantitative target error determination thus enabling the comparison of user algorithms. In closing, while challenges have been forthcoming in many areas, we believe this is the first within the context of image-to-physical liver registration.

Acknowledgements: This work was supported by the National Institutes of Health with award R01CA162477 from the National Cancer Institute, and training grant program T32EB021937 from the National Institute for Biomedical Imaging and Bioengineering.

REFERENCES

[1] J. A. Collins, J. A. Weis, J. S. Heiselman, L. W. Clements, A. L. Simpson, W. R. Jarnagin, *et al.*, "Improving Registration Robustness for Image-Guided Liver Surgery in a Novel Human-to-Phantom Data Framework," *Ieee Transactions on Medical Imaging,* vol. 36, pp. 1502-1510, Jul 2017.

[2] K. Tanaka, H. Shimada, Y. Nagano, I. Endo, H. Sekido, and S. Togo, "Outcome after hepatic resection versus combined resection and microwave ablation for multiple bilobar colorectal metastases to the liver," *Surgery,* vol. 139, pp. 263-273, 2006.

[3] T. Mizuno, J. M. Cloyd, K. Omichi, Y. S. Chun, C. Conrad, C. W. D. Tzeng, *et al.*, "Two-Stage Hepatectomy vs One-Stage Major Hepatectomy with Contralateral Resection or Ablation for Advanced Bilobar Colorectal Liver Metastases," *Journal of the American College of Surgeons,* vol. 226, pp. 825-834, May 2018.

[4] P. C. Giulianotti, A. Coratti, F. Sbrana, P. Addeo, F. M. Bianco, N. C. Buchs, *et al.*, "Robotic liver surgery: Results for 70 resections," *Surgery,* vol. 149, pp. 29-39, Jan 2011.

[5] D. Daskalaki, R. Gonzalez-Heredia, M. Brown, F. M. Bianco, I. Tzvetanov, M. Davis, *et al.*, "Financial Impact of the Robotic Approach in Liver Surgery: A Comparative Study of Clinical Outcomes and Costs Between the Robotic and Open Technique in a Single Institution," *Journal of Laparoendoscopic & Advanced Surgical Techniques,* vol. 27, pp. 375-382, Apr 2017.

[6] J. Hallet, A. S. Cunha, D. Cherqui, B. Gayet, D. Goere, P. Bachellier, *et al.*, "Laparoscopic Compared to Open Repeat Hepatectomy for Colorectal Liver Metastases: a Multi-institutional Propensity-Matched Analysis of Short- and Long-Term Outcomes," *World Journal of Surgery,* vol. 41, pp. 3189-3198, Dec 2017.

[7] S. G. Delis and C. Dervenis, "Selection criteria for liver resection in patients with hepatocellular carcinoma and chronic liver disease," *World J Gastroenterol,* vol. 14, pp. 3452-60, Jun 14 2008.

[8] E. G. Yegin, E. Oymaci, E. Karatay, and A. Coker, "Progress in surgical and nonsurgical approaches for hepatocellular carcinoma treatment," *Hepatobiliary & Pancreatic Diseases International,* vol. 15, pp. 234-256, Jun 2016.

[9] C. O. Laura, K. Drechsler, S. Wesarg, and R. Bale, "Accurate Physics-Based Registration for the Outcome Validation of Minimal Invasive Interventions and Open Liver Surgeries," *Ieee Transactions on Biomedical Engineering,* vol. 64, pp. 362-371, Feb 2017.

[10] I. Peterlik, H. Courtecuisse, R. Rohling, P. Abolmaesumi, C. Nguan, S. Cotin, *et al.*, "Fast elastic registration of soft tissues under large deformations," *Medical Image Analysis,* vol. 45, pp. 24-40, Apr 2018.

[11] R. Plantefeve, I. Peterlik, and S. Cotin, "Intraoperative Biomechanical Registration of the Liver: Does the Heterogeneity of the Liver Matter?," *Irbm,* vol. 39, pp. 18-25, Feb 2018.

[12] R. Plantefeve, I. Peterlik, N. Haouchine, and S. Cotin, "Patient-Specific Biomechanical Modeling for Guidance During Minimally-Invasive Hepatic Surgery," *Annals of Biomedical Engineering,* vol. 44, pp. 139-153, Jan 2016.

[13] D. Reichard, D. Hantsch, S. Bodenstedt, S. Suwelack, M. Wagner, H. Kenngott, *et al.*, "Projective biomechanical depth matching for soft tissue registration in laparoscopic surgery," *International Journal of Computer Assisted Radiology and Surgery*, vol. 12, pp. 1101-1110, Jul 2017.

[14] M. R. Robu, J. Ramalhinho, S. Thompson, K. Gurusamy, B. Davidson, D. Hawkes, *et al.*, "Global rigid registration of CT to video in laparoscopic liver surgery," *International Journal of Computer Assisted Radiology and Surgery*, vol. 13, pp. 947-956, Jun 2018.

[15] L. W. Clements, J. A. Collins, J. A. Weis, A. L. Simpson, L. B. Adams, W. R. Jarnagin, *et al.*, "Evaluation of model-based deformation correction in image-guided liver surgery via tracked intraoperative ultrasound," *Journal of Medical Imaging*, vol. 3, Jan-Mar 2016.

[16] L. W. Clements, J. A. Collins, J. A. Weis, A. L. Simpson, T. P. Kingham, W. R. Jarnagin, *et al.*, "Deformation correction for image guided liver surgery: An intraoperative fidelity assessment," *Surgery*, vol. 162, pp. 537-547, Sep 2017.

[17] L. W. Clements, W. C. Chapman, B. M. Dawant, R. L. Galloway, and M. I. Miga, "Robust surface registration using salient anatomical features for image-guided liver surgery: Algorithm and validation," *Medical Physics*, vol. 35, pp. 2528-2540, Jun 2008.

[18] J. S. Heiselman, L. W. Clements, J. A. Collins, J. A. Weis, A. L. Simpson, S. K. Geevarghese, *et al.*, "Characterization and correction of intraoperative soft tissue deformation in image-guided laparoscopic liver surgery," *Journal of Medical Imaging*, vol. 5, Apr 2018.

[19] D. C. Rucker, Y. F. Wu, L. W. Clements, J. E. Ondrake, T. S. Pheiffer, A. L. Simpson, *et al.*, "A Mechanics-Based Nonrigid Registration Method for Liver Surgery Using Sparse Intraoperative Data," *Ieee Transactions on Medical Imaging*, vol. 33, pp. 147-158, Jan 2014.

[20] L. W. Clements, P. Dumpuri, W. C. Chapman, B. M. Dawant, R. L. Galloway, and M. I. Miga, "Organ Surface Deformation Measurement and Analysis in Open Hepatic Surgery: Method and Preliminary Results From 12 Clinical Cases," *Ieee Transactions on Biomedical Engineering*, vol. 58, Aug 2011.